ARTICLE IN PRESS

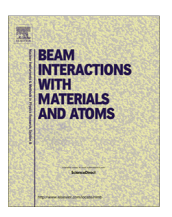
Nuclear Instruments and Methods in Physics Research B xxx (2017) xxx-xxx



Contents lists available at ScienceDirect

Nuclear Instruments and Methods in Physics Research B

journal homepage: www.elsevier.com/locate/nimb



The Raman effects in γ -LiAlO $_2$ induced by low-energy Ga ion implantation

Jing Zhang, Hong-Lian Song, Mei Qiao, Tie-Jun Wang, Xiao-Fei Yu, Xue-Lin Wang*

School of Physics, State Key Laboratory of Crystal Materials and Key Laboratory of Particle Physics and Particle Irradiation (MOE), Shandong University, Jinan 250100, PR China

ARTICLE INFO

Article history:
Received 8 December 2016
Received in revised form 23 April 2017
Accepted 5 May 2017
Available online xxxx

Keywords: Ion implantation Optical material Raman spectroscopy

ABSTRACT

The tetragonal γ -LiAlO $_2$ crystal, known as a promising solid breeding material in future fusion reactors, has attracted much attention for its irradiation effects. This work focused on the Raman effects in ionimplanted γ -LiAlO $_2$. Ga ions of 30, 80 and 150 keV were implanted on the z-cut γ -LiAlO $_2$ sample surfaces at a fluence of $1 \times 10^{14} \, \mathrm{ions/cm^2}$ or $1 \times 10^{15} \, \mathrm{ions/cm^2}$. The average ion range varied from 230 to 910 Å. The Raman spectra were collected from the implanted surfaces before and after the implantation. Evident changes were reflected in the Raman modes intensities, with abnormal increments for the most detected modes. According to the assignments of Raman modes, the Al-O vibration was enhanced to a greater extent than the Li-Al-O vibration, and the LiO $_4$ -AlO $_4$ vibration gained a lesser enhancement. The discussion, including the factors of roughness, crystalline disorder and influence by Ga ions, attempts to explain the increments of Raman intensity.

© 2017 Published by Elsevier B.V.

1. Introduction

Tetragonal γ -LiAlO₂ is a positive uni-axial crystal, the crystalline structure of which can be simply described as Li⁺ and Al³⁺ alternately occupying the center of the oxygen tetrahedron, resulting in the symmetry of space group $P4_12_12$ [1]. γ -LiAlO₂ has many applicable properties, such as small lattice mismatch with III-V semiconductors [2], high sound wave velocities and piezoelectric response [3], and high sensitivity to luminescence [4], among others. However, it is most known as a promising solid breeding material in future fusion reactors [5]. This has attracted various studies to its irradiation effects. Many irradiation sources were applied, for example, neutron [6], electronic [7], x-rays and γ rays [8], and energetic ions [9–11], among others. Characterization methods, such as optical absorption, electron paramagnetic resonance and luminescence spectra, have been reported on the defects and microstructure changes for ion-implanted γ -LiAlO₂ [12–14]. In this work, Raman spectroscopy joins the ranks of techniques characterizing γ-LiAlO₂ with the metal ion implantation method. Raman spectroscopy was used to present Li ion diffusion in LiAlO₂ at different temperatures, and the corresponding Raman mode assignments were tentatively given with the references of respectable previous works [15-17]. We followed the assignments and

2. Experimental methods

After being polished and cleaned, z-cut γ -LiAlO₂ crystal samples with dimensions of $7 \times 5 \times 1$ mm supplied by Shanghai Daheng Optics and Fine Mechanics Co., Ltd., a crystal material company, were implanted by 30, 80 and 150 keV Ga ions, respectively, at room temperature under vacuum condition at Institute of Semiconductors, Chinese Academy of Sciences. For each energy level, two fluences of $1 \times 10^{14} \, \mathrm{ions/cm^2}$ and $1 \times 10^{15} \, \mathrm{ions/cm^2}$ were applied in turn. The ion beam was tilted 7° to the normal of a 7×5 mm surface to avoid channeling effects. The Raman spectra of γ -LiAlO₂ on the surfaces were recorded before and after the implantation using a Horiba/Jobin Yvon HR800 micro confocal Raman spectrometer at room temperature. A He-Ne laser with a wavelength of 633 nm was used as an excitation source. The diameter of the laser beam spot focused on the sample surface was approximately 1 μ m.

3. Results and discussion

According to the SRIM (Stopping and Range of Ions in Matter) program simulation [18], the average range of 30, 80 and 150 keV Ga ions in $\gamma\text{-LiAlO}_2$ were 232, 514 and 911 Å, respectively, all in the near-surface range. The fluences of 1 \times 10 14 ions/cm² and

http://dx.doi.org/10.1016/j.nimb.2017.05.013 0168-583X/© 2017 Published by Elsevier B.V.

Please cite this article in press as: J. Zhang et al., The Raman effects in γ -LiAlO₂ induced by low-energy Ga ion implantation, Nucl. Instr. Meth. B (2017), http://dx.doi.org/10.1016/j.nimb.2017.05.013

focused on the changes of the observed Raman modes of γ -LiAlO₂, excluding Li⁺ behavior.

^{*} Corresponding author.

E-mail address: xuelinwang@sdu.edu.cn (X.-L. Wang).

 $1\times10^{15}\,\text{ions/cm}^2$ induced the maximum dpa (displacements per atom) in the order of 0.1 and 1.0, respectively. Although the dpa do not include the recovery of displaced atoms, we could still deduce that the disorder would cover the Ga-implanted surface partially or almost completely. Additionally, the sputtering effects were not evaluated in this work.

The Raman spectra of $\gamma\text{-LiAlO}_2$ sample surfaces are listed in Fig. 1. Fig. 1(a) demonstrated the surface Raman spectroscopy of samples before implantation and after the implantation by 30 keV Ga ions at a fluence of $1\times10^{14}\,\text{ions/cm}^2$ and at a fluence of $1\times10^{15}\,\text{ions/cm}^2$. Owing to the accuracy of experiments and the imperfect crystals, there were only nine observed modes:

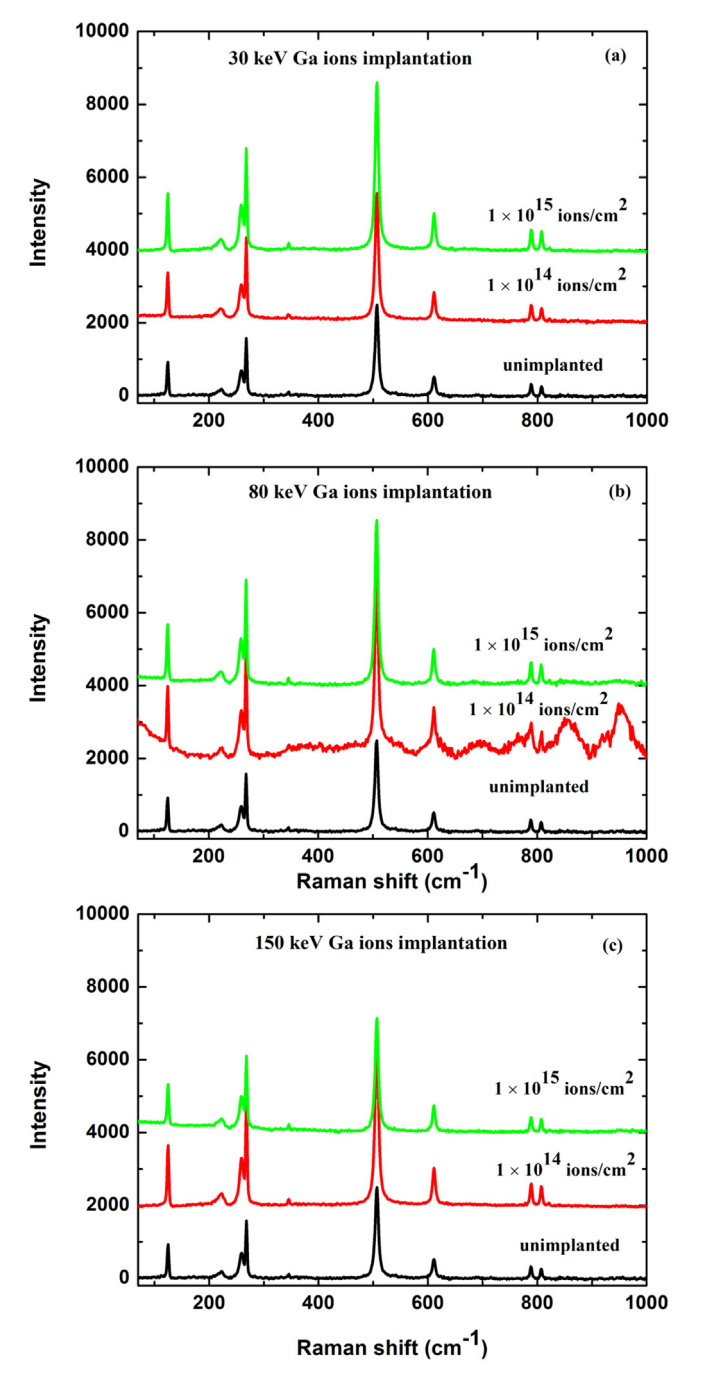


Fig. 1. Raman spectra of the sample surface before and after the implantation at fluences of $1\times10^{14}\,\text{ions/cm}^2$ and $1\times10^{15}\,\text{ions/cm}^2$: (a) 30 keV Ga ions; (b) 80 keV Ga ions; and (c) 150 keV Ga ions.

 $125\,\mathrm{cm}^{-1}$ $(B_2^{(1)},\ \text{LiO}_4\text{-AlO}_4),\ 222\,\mathrm{cm}^{-1}$ $(B_2^{(2)},\ \text{Li-O}$ stretching), $259\,\mathrm{cm}^{-1}$ $(B_1^{(1)},\ \text{Li-O-Al}$ stretching), $268\,\mathrm{cm}^{-1}$ $(B_2^{(3)},\ \text{Li-O-Al}$ stretching), $345\,\mathrm{cm}^{-1}$ $(E^{(2)},\ \text{Li-O}$ bending), $507\,\mathrm{cm}^{-1}$ $(E^{(3)},\ \text{Al-O}$ bending), $611\,\mathrm{cm}^{-1}$ $(E^{(4)},\ \text{Al-O}$ bending), $789\,\mathrm{cm}^{-1}$ $(B_2^{(4)},\ \text{Al-O}$ stretching) and $807\,\mathrm{cm}^{-1}$ $(B_1^{(4)},\ \text{Al-O}$ stretching), all of which are listed in Table 1. In Table 1, the detected Raman modes are listed corresponding to the experiment and calculation results of the Ref. [15]. The difference was no more than $2\,\mathrm{cm}^{-1}$ between the two experimental modes, except for the $345\,\mathrm{cm}^{-1}$ mode. However, when looking at the difference in the $789\,\mathrm{cm}^{-1}$ mode between the experimental and calculated results, the assignment of the $345\,\mathrm{cm}^{-1}$ mode to $E^{(2)}$ could be reasonable.

As shown in Fig. 1(a), changes mainly occurred in mode intensities, especially for the strongest peak $507~\rm cm^{-1}$. The intensity of the $507~\rm cm^{-1}$ mode tended to increase with increasing fluences. In Fig. 1(b), for 80 keV Ga ion implantation, similar increments of intensity occurred to the strongest peak at the two fluences. The different behavior of the Raman spectrum of the sample implanted at a fluence of $1\times 10^{14}~\rm ions/cm^2$ may reflect of the local differences of the surface. However, in Fig. 1(c), for 150 keV Ga ion implantation, the increment of the strongest peak intensity decreased with increasing fluences.

Specifically, we outlined several Raman modes and marked the relatively increased proportion of intensity in Fig. 2. Fig. 2(a)-(e) shows the relationship between the increased proportion of the Raman mode intensity and the implanted energy at the two fluences for 125, 259, 268, 507, and 611 cm⁻¹. As to the rest four modes of the nine, the corresponding intensities also increased in different proportion. As shown in Fig. 2(a)-(e), the intensities of the five marked modes increased to different degrees. In Fig. 2(a), for the 30 keV ion implantation, there was a positive difference between the increments of the 125 cm⁻¹ mode intensities at the higher fluence of $1 \times 10^{15} ions/cm^2$ and the lower fluence of 1×10^{14} ions/cm². The positive difference of the two increments decreased to almost zero for the 80 keV ion implantation, and it became negative for the 150 keV ion implantation. From another point of view, the increment of the 125 cm⁻¹ mode intensity increased with increasing implanted energy at a fluence of $1 \times 10^{14} \, \text{ions/cm}^2$ and reduced with increasing implanted energy at a fluence of 1×10^{15} ions/cm². Two different trends intersected at approximately 80 keV. Similar conclusions could be drawn from Fig. 2(b)-(e). Note that, at 80 keV, the difference of the two incre-

Table 1 Observed modes of γ -LiAlO $_2$ sample and the corresponding experimental and calculated results from the Ref. [15].

Observed Modes (cm ⁻¹)	Experimental Modes (cm ⁻¹) [15]	Calculated Modes (cm ⁻¹) [15]	Assignments [15]
125	124	117	$B_2^{(1)}$, LiO ₄ -AlO ₄
222	220	230	B ₂ ⁽²⁾ , Li-O
			stretching
259	260	270	B ₁ ⁽¹⁾ , Li-O-Al
			stretching
268	268	278	B ₂ ⁽³⁾ , Li-O-Al
			stretching
345	366	382	E ⁽²⁾ , Li-O
			bending
507	508	494	E ⁽³⁾ , Al-O
			bending
611	613	625	E ⁽⁴⁾ , Al-O
700	704	707	bending
789	791	737	B ₂ ⁽⁴⁾ , Al-O
		=	stretching
807	809	793	B ₁ ⁽⁴⁾ , Al-O
			stretching

Download English Version:

https://daneshyari.com/en/article/5467226

Download Persian Version:

https://daneshyari.com/article/5467226

<u>Daneshyari.com</u>